Intracranial Displacements due to Blunt Force Impact in a Post-Mortem Human Surrogate Brain

J Demiannay, J Rovt, M Brannen, S Xu, G Kang, A Yip, A H Azadi, P Dehghan, S Goodwin, R Taylor, K Poon, S Brien, C Karton, B Hoshizaki, O Petel

I. INTRODUCTION

The prediction and prevention of mild traumatic brain injury (mTBI) is reliant on understanding the biomechanical response of the brain to external stimuli. Rotational motion and acceleration, along with accompanying brain tissue deformation and strains, are likely primary mechanisms for mTBI. Increasingly, finite element (FE) models are being used to study the deformation and strains that occur in brain tissue due to blunt-force impacts to assess brain injury risk. FE head injury models are typically validated using brain-skull deformation measurements [1-2] from post-mortem human subjects (PMHS) [3-5]. Analysis of these models has indicated that current PMHS datasets may not be sufficient for accurate FE model validation and additional regional PMHS intracranial displacement and strain datasets would be beneficial for accurate injury risk assessment in FEM [2]. In this study, the responses of four PMHS heads were recorded using a high-speed X-ray (HSXR) imaging system after being subjected to blunt force impacts. The objective of this research is to: (a) measure the brain-skull relative deformations and strains that occur as a result of blunt force impacts; (b) target anatomical regions within the brain to determine how each region responds; (c) investigate the brain's biomechanical response to different impact conditions, including varying linear and rotational accelerations, impactor compliance, and impact location.

II. METHODS

Three PMHS specimens were subjected to a total of 18 frontal impacts, and one specimen was subjected to 12 rear impacts. Linear and rotational acceleration data was collected using a 6-axis accelerometer (6DX PRO 2k-18k SLICE, Diversified Technical Systems Inc.), and brain-skull relative deformation was measured using the HSXR imaging system. Radiopaque 2.75 mm elastomeric markers were implanted along the parasagittal plane into the brain tissue of each specimen, targeting 10 anatomical regions. The marker stiffness, density, and spacing were optimised to minimise interference with the deformation of the brain tissue and maintain biofidelity [6]. The markers were embedded using a custom cannula rig to prevent coring and minimise damage to the surrounding tissue during marker insertion. Markers were inserted within a parasagittal plane (15 mm from sagittal), and a secondary parasagittal plane (5 mm from sagittal) to target the brain stem and corpus callosum. The specimens were then attached to a mechanical neck without directional bias and mounted to the impact table coupled to the HSXR imaging system. The specimens were impacted in an upright configuration, as boundary conditions may change with posing of the head [7], to improve biofidelity [5]. Careful attention was given to ensuring that the specimens were properly perfused with artificial cerebrospinal fluid (aCSF) to improve biofidelity, with direct filling of the ventricular and subdural spaces. The specimens were perfused to maintain a constant pressure of 1000 mmH_2O during impacts, and X-ray images of the specimens were used to ensure that no visible air pockets remained in the specimen skulls. The specimens were subjected to impacts using a linear impactor with two possible end caps, a neoprene (low compliance) or VN foam (medium compliance), at impact velocities ranging between 0.9 m/s and 4.9 m/s. The resulting motion of the embedded markers were tracked using the HSXR imaging system at a rate of 5000 frames per second. Post-impact MRIs were used to ensure that the markers were properly embedded within the brain tissue, and the anatomical locations of each marker were verified. The skull-brain relative deformation was then determined by tracking the embedded markers using a custom-built

J. Demiannay (e-mail: jeanjacquesdemiannay@cmail.carleton.ca; tel: +1 613-261-3124) and A. Yip are MASc students, J. Rovt, M. Brannen, S. Xu are PhD students, and O.E. Petel is an Associate Professor in Mechanical & Aerospace Engineering at Carleton University, Ottawa, ON, Canada. A. H. Azadi and P. Dehghan are PhD students, and T. B. Hoshizaki is a Professor of Biomechanics in the School of Human Kinetics at University of Ottawa, Ottawa, ON, Canada. S. Goodwin is a Senior Prosector in the Anatomy Lab at University of Ottawa. R. Taylor is a physicist at The Royal Mental Health Centre in Ottawa, Canada. K. Poon is a Neurosurgeon at the Clinique Neuro-Outaouais in Gatineau, QC, Canada. S. Brien is the Senior Vice President Medical, Academic, and Research Affairs at the Horizon Health Network. C. Karton is a Senior Research Associate at University of Ottawa.

MATLAB program. Strain is then calculated for the anatomical regions of the brain using the displacement measurements of the embedded markers.

III. INITIAL FINDINGS

The displacement of the markers relative to fixed skull frame of reference was tracked over time for each impact. Specimens CO-106, CO-107, and CO-108 were subjected to frontal impacts, and specimen CO-109 was subjected to rear impacts using the linear impactor. Figure 1 shows a comparison of marker displacements over time of a frontal and rear impact with same impactor cap (75 mm of VN foam) and similar impact velocities of 4.0 m/s and 3.9 m/s, respectively. The marker displacement profiles shown are for the first 100 ms following impact, showing the specimen range of motion for the full initial counterclockwise rotation and following clockwise counter rotation. Table I gives a summary of the peak linear and rotational acceleration, and rotational rate for the impacts shown in Fig. 1

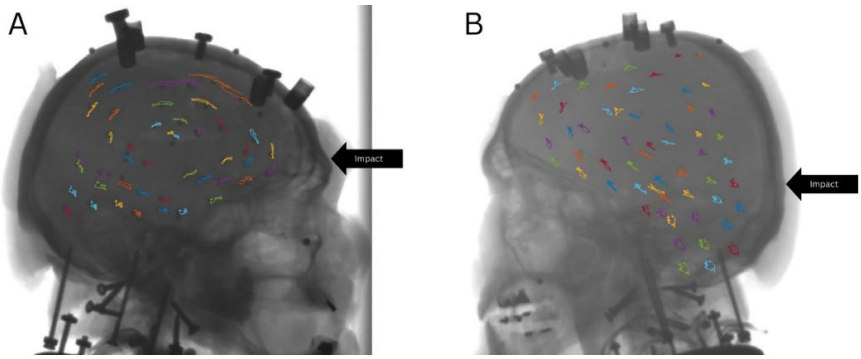

Fig. 1. Marker displacements paths for the first 100 ms following impact, overlaid on X-ray images of the PMHS specimens. Arrow indicates direction and location of impact. (A) Specimen CO-108, results for a front impact with a VN foam impactor cap at a velocity of 4.0 m/s. (B) Specimen CO-109, results for a rear impact with a VN foam impactor cap at a velocity of 3.9 m/s

TABLE I
IMPACT VELOCITY, PEAK LINEAR ACCELERATION, PEAK ROTATIONAL VELOCITY AND ACCELERATION FOR CO-108 AND CO-109

Specimen Number	Impact Velocity (m/s)	Peak Linear Acceleration at CG (g)	Peak Rotational Velocity (rad/s)	Peak Rotational Acceleration (rad/s^2)	Peak displacement (mm)
CO-108	4.0	60.6	19.7	2343	8.2
CO-109	3.9	158.4	20.5	5653	5.7

IV. DISCUSSION

A comparison of the brain motion resulting from the frontal and rear impacts demonstrated that the direction of impact, as well as anatomical location, had significant effects on relative brain-skull displacements. The brain deformation profiles in the two impact scenarios were markedly different, as interaction with boundary conditions changed based on the impact orientation. If we analyse the motion based on region, the frontal and parietal regions exhibited less anterior-posterior motion from a rear impact, while the occipital region exhibited more anterior-posterior motion from the rear impact. The cerebellum had increased superior-inferior motion in the rear impact orientation as compared to prior frontal impacts. Overall, the rear impact tests have shown comparatively lower peak displacement in the majority of the regions of the brain examined, with the exception of the cerebellum, despite the higher peak accelerations (Table I). During frontal impacts the highest displacements occurred near the location of impact, while rear impacts exhibited lower displacements near the location of impact. Most importantly, while prior work has shown that the brain rotated about its centre of gravity during a frontal impact [5], this does not appear to be the case in a rear impact event. The data acquired from this study provide further insights into the biomechanical response of the brain when subjected to blunt impact.

V. REFERENCES

[1] Zhou, Z., *et al*., *Stapp Car Crash J*, 2018.
[2] Zhao, W., *et al*., *Ann Biomed Eng*, 2020.
[3] Hardy, W. N., *et al*., *Stapp Car Crash J*, 2007.
[4] Alshareef, A., *et al*., *J Neurotrauma*, 2020.
[5] Dutrisac, S., *et al.*, *Ann Biomed Eng*, 2021.
[6] Dutrisac, S., *et al*., *J Biomech Eng*, 2021.
[7] Rice, J., *et al*., *NeuroImage*, 2013.